Engineering Inverted Architecture Colloidal Quantum Dot Solar Cells

Dana Kachman[1], Arlene Chiu[1], Susanna M. Thon[1]
[1]Department of Electrical and Computer Engineering
Johns Hopkins University

Abstract

Motivation.

- Colloidal quantum dots (CQDs) are a promising material for use in solar cells because their band gap can be tuned by tuning the CQD size
- Currently, the hole transport layer (HTL) is limiting the performance of CQD solar cells, and 2D WSe_2 is a promising candidate as a replacement HTL
- 2D WSe_2 cannot easily be incorporated into the standard CQD solar cell architecture because many deposition methods use either high temperatures or aqueous solutions, both of which can damage CQD films
- In an inverted architecture device, the HTL is deposited before the CQD absorbing layer, enabling us to more easily deposit 2D WSe_2 without damaging the CQDs

Methods.

Simulations: SCAPS-1D[1], transfer matrix method (TMM) calculations[2]

Fabrication: Colloidal synthesis, spin-casting, evaporation

Measurements: Illuminated current-voltage (JV) testing

Results.

- SCAPS/TMM simulations of device performance show that an optimized inverted device can almost match the performance of a standard device
- TMM calculations show increased absorption in the HTL of an inverted device which is a reason for the marginally decreased performance seen in an inverted device
- We experimentally demonstrated a working inverted CQD solar cell and are now optimizing the performance

Introduction

The structure of a standard CQD solar cell is as follows, starting from the glass substrate side: transparent conductive electrode, electron transport layer (ETL), absorbing layer, hole transport layer (HTL), top electrode. For an inverted device, the location of the HTL and ETL are switched. Additionally, the contact materials are changed[3]. Both structures are shown in Figure 1a below.

The standard materials are as follows: indium or fluorine tin oxide (ITO/FTO) as the transparent conductive electrode, ZnO nanoparticles as the ETL, PbX_2-capped PbS CQDs (where X = I and Br) as the absorbing layer, 1,2-ethanedithiol (EDT) capped PbS CQDs as the HTL, and Al or Au as the top electrode.

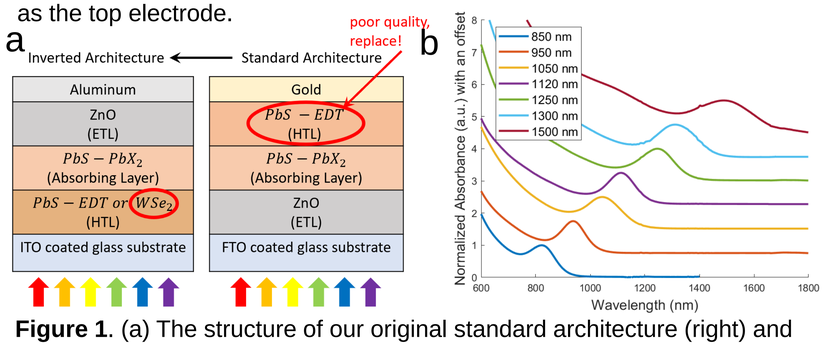

Figure 1. (a) The structure of our original standard architecture (right) and our goal for the inverted architecture device (left). (b) The absorbance spectra of CQDs of different sizes.

Transfer Matrix Method (TMM) Calculations

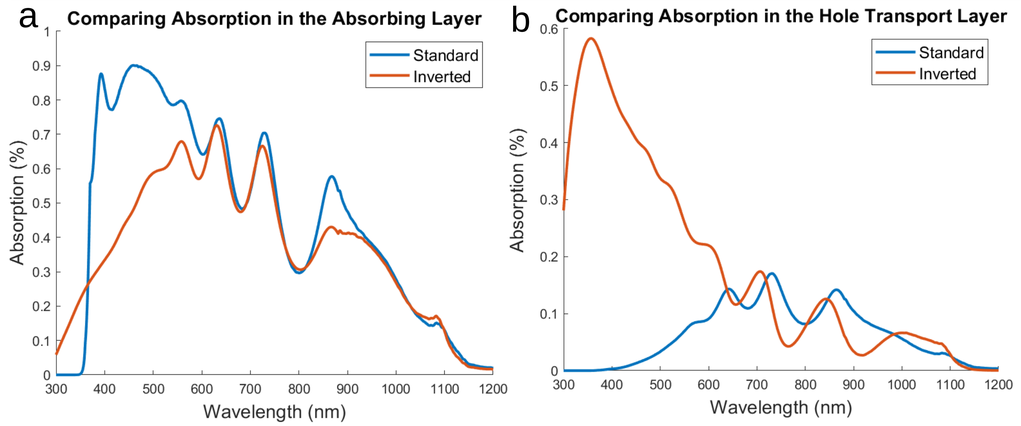

Figure 2. (a) Absorption in the absorbing layer (PbS-PbX_2) and (b) absorption in the HTL (PbS-EDT) are compared for the standard (red) and inverted (blue) architectures.

Efficiency is maximized when a higher proportion of light is absorbed within the absorbing layer.

Because the current HTL is made of CQDs, which absorb light strongly, there can be significant absorption in the HTL, hurting the solar cell's efficiency.

This effect is more pronounced in an inverted device, especially at shorter wavelengths. This is because in an inverted device the HTL is closer to the illumination plane (vs. farther away from the illumination plane in the standard architecture).

Our goal to use $2D\ WSe_2$ as the HTL should address this issue because it's very thin, reducing the amount of absorbance as compared to our current CQD HTL. Simulations and device fabrication to investigate the performance of WSe_2 as an HTL are ongoing.

SCAPS/TMM Simulations

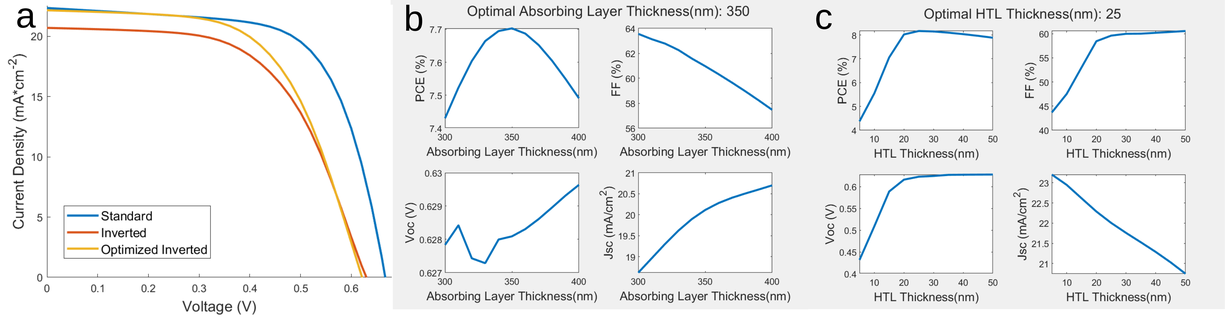

Figure 3. (a) JV curves of the standard (blue), inverted (red), and optimized inverted (yellow) architectures using SCAPS/TMM simulation sweeps of (b) absorbing layer and (c) HTL thickness.

For these simulations, TMM calculations were used to produce photogeneration rates for the structure. This information was then input to SCAPS simulations to produce the data for the JV curves.

Device Testing

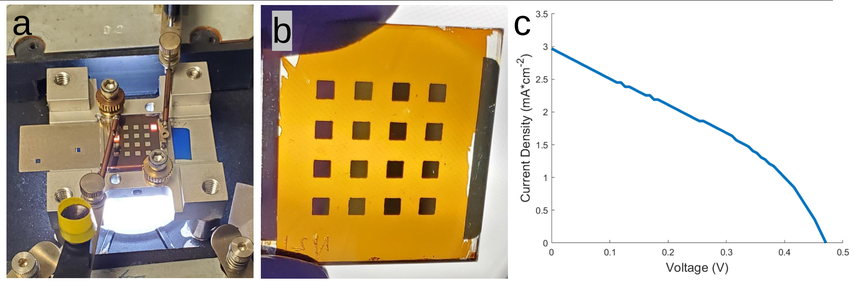

Figure 4. (a) The device testing set up. (b) An image of a fully fabricated standard solar cell array. (c) A JV curve for a working inverted CQD solar cell.

We produced a working inverted solar cell using the architecture shown in Figure 1a. It achieved an initial power conversion efficiency of 0.5%. Optimization work is ongoing to improve the performance.

References

(1) Burgelman, M.; Nollet, P.; Degrave, S. Modelling Polycrystalline Semiconductor Solar Cells. Thin Solid Films 2000, 361−362, 527−532.

(2) Burkhard, G. F.; Hoke, E. T.; McGehee, M. D. Accounting for Interference, Scattering, and Electrode Absorption to Make Accurate Internal Quantum Efficiency Measurements in Organic and Other Thin Solar Cells. Adv. Mater. 2010, 22, 3293−3297.

(3) Wang, R. L., Wu, X., Xu, K., Zhou, W., Shang, Y., Tang, H., Chen, H., Ning, Z., Adv. Mater. 2018, 30, 1704882. https://doi.org/10.1002/adma.201704882

Acknowledgements

This work was funded by the National Science Foundation (DMR-1807342) and the Department of Defense Center for Excellence in Advanced Electro-Photonics with 2D Materials (Cooperative Agreement Number: W911NF2120213).